

Gauge problem of monopole dynamics in SU(2) lattice gauge theory

メタデータ	言語: eng 出版者: 公開日: 2017-10-05 キーワード (Ja): キーワード (En): 作成者: メールアドレス: 所属:
URL	https://doi.org/10.24517/00028517

This work is licensed under a Creative Commons Attribution-NonCommercial-ShareAlike 3.0 International License.



Gauge problem of monopole dynamics in $SU(2)$ lattice gauge theory

Shoichi Ito,¹ Shun-ichi Kitahara,² Tae Woong Park,¹ and Tsuneo Suzuki¹
¹*Institute for Theoretical Physics, Kanazawa University, Kanazawa 920-1192, Japan*
²*Jumonji University, Niiza, Saitama 352-8510, Japan*

(Received 24 December 2002; published 15 April 2003)

The gauge problem of monopole dynamics is studied in $SU(2)$ lattice gauge theory. We study first the Abelian and monopole contributions to the static potential in four smooth gauges, i.e., the Laplacian Abelian, maximally Abelian Wilson loop, and L -type gauges in comparison with the maximally Abelian (MA) gauge. They all reproduce the string tension in good agreement with the $SU(2)$ string tension. The MA gauge is not the only choice of a good gauge which is suitable for the color confinement mechanism. Using an inverse Monte Carlo method and block spin transformation, we determine the effective monopole actions and the renormalization group (RG) flows of its coupling constants in various Abelian projection schemes. Every RG flow appears to converge to a unique curve which suggests gauge independence in the infrared region.

DOI: 10.1103/PhysRevD.67.074504

PACS number(s): 12.38.Gc, 11.15.Ha

I. INTRODUCTION

It is important to understand the color confinement mechanism in quantum chromodynamics (QCD). Many numerical simulations have been done and they support the dual superconductor scenario of the QCD vacuum as a confinement mechanism [1,2]. Magnetic monopoles are induced by performing an Abelian projection [3], i.e., a partial gauge fixing that keeps $U(1) \otimes U(1)$. It is known that the string tension calculated from the Abelian and the monopole parts reproduces well the original one when we perform an Abelian projection in the maximally Abelian (MA) gauge where link variables are Abelianized as much as possible. In addition to the string tension, many low-energy physical properties of QCD are reproduced from the Abelian and monopole degrees of freedom alone. It is called ‘‘Abelian and monopole dominance.’’ These facts suggest that monopoles play an important role for the confinement mechanism. Actually, a low-energy effective theory that is described in terms of monopole currents has been derived by Shiba and Suzuki [4] and an almost perfect monopole action showing the scaling behavior has been derived by Chernodub *et al.* [5]. Monopole condensation occurs due to energy-entropy balance [4]. The Abelian color-electric flux is squeezed into a stringlike shape [6,7] by the superconducting monopole current. This squeezed color flux causes a confinement potential between quarks.

We note that we have infinite degrees of freedom when we perform an Abelian projection. That is to say, which gauge should be chosen? Recently the Laplacian Abelian (LA) gauge was proposed and it appears to have similar good properties [8,9]. Actually the MA and LA gauges are very similar. Are the MA and LA gauges exceptional? If such is the case, there must exist a reason to justify it, although it seems very difficult to find this reason. Another interpretation is that monopole dynamics does not depend on the choice of gauge in the continuum limit, although it seems dependent on the gauge choice at the present stage of lattice study. In other words, the MA gauge and LA gauge are considered to have a wider window even at present to see the continuum limit than other gauges.

Our aim in this paper is to show first that the MA gauge is not a special choice of a good gauge for color confinement. We restrict ourselves to pure $SU(2)$ QCD for simplicity. Here we discuss two new gauges in addition to the LA gauge. They have a different continuum limit but they can all reproduce well the $SU(2)$ string tension. The second aim is to derive an effective monopole action and to study the block spin transformation of the monopole currents in various Abelian projections. If their renormalization group (RG) flows converge onto the same line with a finite number of block spin transformations, we can expect gauge independence of monopole dynamics in the infrared region. The paper is organized as follows. In Sec. II, we present some theoretical and phenomenological arguments which support gauge independence of Abelian and monopole dominance. In Sec. III, we describe by gauge fixing procedures being used. In Sec. IV, we show that the $SU(2)$ string tension is well reproduced from Abelian or monopole degrees of freedom alone in four different Abelian projection schemes. In Sec. V, we present our results from RG flow study of effective monopole actions in various Abelian projections. In Sec. VI, we summarize our conclusions.

II. THEORETICAL AND PHENOMENOLOGICAL BACKGROUND

A. Gauge fixings and Abelian dominance

It is known that the Abelian Wilson loop reproduces well the $SU(2)$ string tension numerically, if the MA or LA gauge is applied [9,10]. In the case of the Polyakov gauge, the string tension which is calculated from Abelian Polyakov loop correlators is exactly the same as that of $SU(2)$ [11]. Shoji *et al.* developed a stochastic gauge fixing method which interpolates between the MA gauge and no gauge fixing [12]. They found that Abelian dominance for the heavy quark potential is realized even in a gauge that is far from the MA gauge. In a finite temperature system, Abelian Polyakov loops in various gauges reproduce the phase transition behavior of the $SU(2)$ Polyakov loop [13] (see Fig. 1).

Abelian dominance is also shown analytically. Abelian Wilson loops constructed without any gauge fixing give the

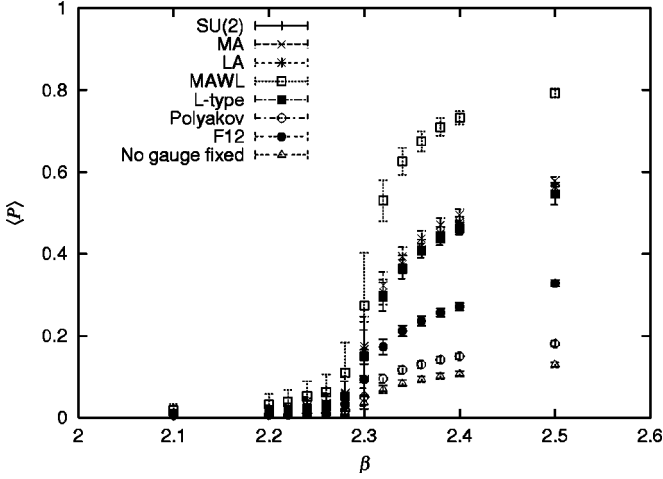


FIG. 1. $SU(2)$ Polyakov loop vs Abelian Polyakov loop in various gauges. The behavior of the $SU(2)$ Polyakov loop is well reproduced by the Abelian Polyakov loop in these gauges.

same string tension as that of $SU(2)$ Wilson loops in the strong coupling expansion [10]. The same fact for any coupling region has been proved by Ogilvie using the character expansion [14]. An Abelian Wilson loop operator is given by

$$W_A[C] = \frac{1}{2} \text{Tr} \left[\prod_{s, \mu \in C} u_\mu(s) \right],$$

where u_μ is an Abelian projected $U(1)$ link variable. Since W_A is not a class function of the $SU(2)$ group, only the $SU(2)$ invariant part extracted from W_A is nonvanishing in the expectation value. This can be written as

$$W_A^{inv} = \frac{1}{2} \int \mathcal{D}g \text{Tr} \left[\prod_{s, \mu \in C} g(s) u_\mu(s) g^\dagger(s + \hat{\mu}) \right].$$

Using a character expansion, we get an expression for the expectation value of the Abelian Wilson loop in terms of $SU(2)$ Wilson loops:

$$\langle W_A^{inv} \rangle = \left(\frac{2}{3} \right)^{P(C)} \langle W_{SU(2)} \rangle_{1/2} + (\text{half integer higher representations}).$$

Since the lowest representation is dominant, we can show that the $SU(2)$ string tension $\sigma_{SU(2)}$ can be reproduced perfectly from the Abelian string tension σ_A :

$$\sigma_A = - \lim_{I, J \rightarrow \infty} \ln \frac{\langle W_A(I+1, J+1) \rangle \langle W_A(I, J) \rangle}{\langle W_A(I+1, J) \rangle \langle W_A(I, J+1) \rangle} = \sigma_{SU(2)}.$$

Furthermore, Ogilvie has shown that similar arguments hold even with the gauge fixing function

$$S_{gf} = \lambda \sum \text{Tr} [U_\mu(s) \sigma_3 U_\mu^\dagger(s) \sigma_3],$$

if the gauge parameter λ is small enough.

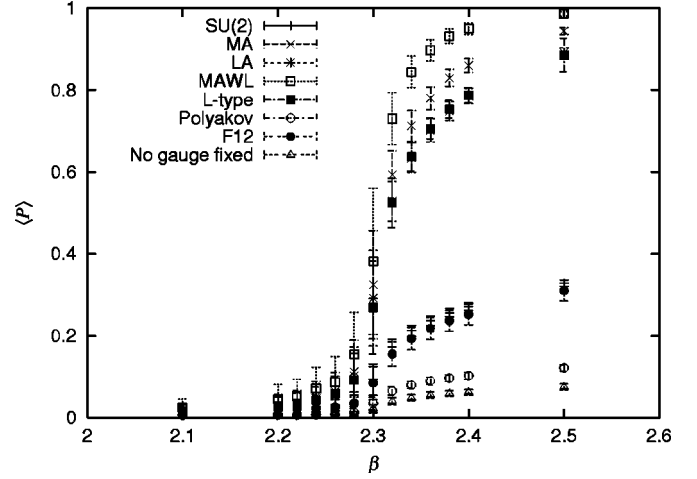


FIG. 2. $SU(2)$ Polyakov loop vs monopole Polyakov loop in various gauges. The behavior of the $SU(2)$ Polyakov loop is well reproduced by the monopole Polyakov loop in these gauges.

B. Monopole dominance

There are numerical results supporting monopole dominance. $SU(2)$ string tension is well reproduced only from the monopole part of Abelian Wilson loops in the MA gauge [15,16] and LA gauge [9]. We note also that monopole Polyakov loops in various gauges reproduce the phase transition behavior of the $SU(2)$ Polyakov loop [13] (see Fig. 2).

In addition to this numerical evidence, we can prove analytically the gauge independence of monopole dominance if Abelian dominance is gauge independent [17]. If Abelian dominance is gauge independent, a common Abelian effective action S_{eff} written in terms of the Abelian gauge field surely exists in any gauge and works well in the infrared region as in the MA gauge. Since S_{eff} takes the form of a modified compact QED, an effective monopole action can be derived analytically. One can evaluate the contribution of monopoles to the Abelian Wilson loop using this effective monopole action.

In the MA gauge, it is known numerically that an effective monopole action composed of two-point self + Coulomb + nearest-neighbor interactions is a good approximation in the infrared region. The action can be transformed exactly into a modified compact QED action in the generic Villain form:

$$Z = \int_{-\pi}^{\pi} \mathcal{D}\theta \sum_{n \in \mathbb{Z}} \exp \left[- \frac{1}{4\pi^2} (d\theta + 2\pi n, \Delta D \times (d\theta + 2\pi n) + i(J, \theta)) \right],$$

where $D \sim \beta \Delta^{-1} + \alpha + \gamma \Delta$. The expectation value of the Abelian Wilson loop $W = e^{i(\theta, J)}$ can be estimated using this action, where J is the color electric current which takes the values ± 1 on a closed loop. When we use the Berenskii-Kosterlitz-Thouless (BKT) transformation [18,19], we get the expectation value of the Abelian Wilson loop in terms of monopole currents k :

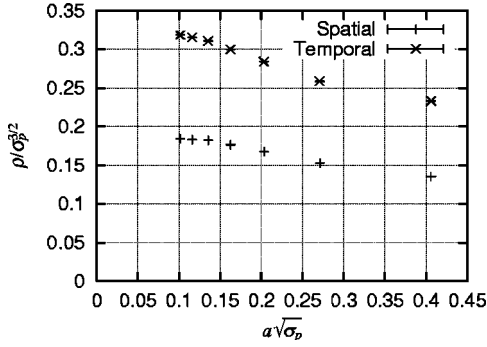


FIG. 3. Monopole density in Polyakov gauge versus lattice spacing.

$$\langle W \rangle = \frac{1}{Z} \sum_{k \in \mathbb{Z}, dk=0} \exp\{- (k, Dk) - 2\pi i (k, \delta \Delta^{-1} M) - \pi^2 [J, (\Delta^2 D)^{-1} J]\}, \quad (1)$$

where M takes the values ± 1 on a surface whose boundary is J ($J = \delta M$). Electric-electric current (J - J) interactions are of a modified Coulomb interaction and have no line singularity leading to a linear potential. The linear potential of the Abelian Wilson loop originates from the second term of the monopole contribution. The gauge independence of monopole dominance is derived from that of Abelian dominance. The gauge independence of an order parameter is also observed in Ref. [20].

C. The objection to gauge independence

As we have shown in previous subsections, there is encouraging evidence that supports gauge independence of the confinement scenario in terms of monopoles. On the other hand, there is a strong objection to the idea of gauge independence.

Consider a gauge called the Polyakov gauge where Polyakov loop operators are diagonalized in continuum finite-temperature QCD. It is proved [21,22] that the singularities of the gauge fixing run only in the timelike direction. This means that there are only timelike monopoles in the system when the Polyakov gauge is employed, if the degeneracy points in Abelian projection correspond only to monopoles as 't Hooft argued. Since such timelike monopoles do not contribute to the physical string tension [23], monopole dominance is violated.

But numerically the above theoretical expectation seems to be inconsistent with numerical data. We show our preliminary result in Fig. 3. The spatial and temporal monopole densities are plotted in Fig. 3 as a function of lattice spacing a in the unit of physical string tension $\sqrt{\sigma_p}$. These densities are defined as

$$\rho_s(\beta) = \frac{\frac{1}{3} \sum_s \sum_{i=1,2,3} |k_i(s)|}{(N_s a)^3 N_4},$$

$$\rho_t(\beta) = \frac{\sum_s |k_4(s)|}{(N_s a)^3 N_4},$$

respectively. Figure 3 shows that the spatial (lattice) monopole density may take nonzero values even in the $a \rightarrow 0$ limit. This is not compatible with the theoretical expectation above. In the authors' opinion, the continuum limit of lattice monopoles must contain extra ingredients different from the expected monopoles corresponding to singularities of Polyakov loop operators. We will give a detailed analysis elsewhere.

III. VARIOUS ABELIAN PROJECTIONS ON A LATTICE

To check gauge (in)dependence of monopole dynamics, we study the Abelian projection in various gauges.

(1) MA gauge. The most well known is the maximally Abelian gauge. It is defined by maximizing the following quantity (R_{MA}):

$$R_{MA} = \text{T} \sum_{s,\mu} U_\mu(s) \sigma_3 U_\mu^\dagger(s) \sigma_3. \quad (2)$$

This is achieved by diagonalizing the operator

$$X_{MA}(s) = \sum_\mu [U_\mu(s) \sigma_3 U_\mu^\dagger(s) + U_\mu^\dagger(s - \hat{\mu}) \sigma_3 U_\mu(s - \hat{\mu})].$$

That is,

$$X_{MA}(s) \rightarrow X'_{MA}(s) = V(s) X_{MA}(s) V^\dagger(s) = \text{diag}\{\lambda_1, \lambda_2\},$$

where $V(s)$ is a gauge transformation matrix. The diagonalization corresponds to the condition

$$\sum_\mu (\partial_\mu \mp i A_\mu^3) A_\mu^\pm = 0 \quad (3)$$

in the continuum limit.

(2) LA gauge [8]. First consider the MA gauge again. To maximize R_{MA} in Eq. (2) is to minimize the functional

$$S_{MA} = \sum_{s,\mu} \left\{ 1 - \frac{1}{2} \text{Tr}[\Phi(s) U_\mu(s) \Phi(s + \hat{\mu}) U_\mu^\dagger(s)] \right\} = \sum_{s,\mu} \{ 1 - \phi^a(s) R_\mu^{ab}(s) \phi^b(s + \hat{\mu}) \}, \quad (4)$$

where R_μ is a gauge field in the adjoint representation,

$$R_\mu^{ab}(s) = \frac{1}{2} \text{Tr}[\sigma_a U_\mu(s) \sigma_b U_\mu^\dagger(s)].$$

Φ is parametrized by a spin variable ϕ which satisfies the local constraint

$$\Phi(s) = V^\dagger(s) \sigma_3 V(s) = \sum_{a=1}^3 \phi^a(s) \sigma_a, \quad (5)$$

$$\sum_{a=1}^3 [\phi^a(s)]^2 = 1. \quad (6)$$

Because of the local constraint from the normalization, it is very difficult to find a set of ϕ which realizes the absolute minimum of Eq. (4).

The key idea of the LA gauge fixing is to relax this constraint:

$$\sum_{a=1}^3 [\phi^a(s)]^2 = 1 \rightarrow \sum_s \sum_{a=1}^3 [\phi^a(s)]^2 = 1.$$

The functional to minimize becomes

$$S_{LA} = \frac{1}{2} \sum_{x,a} \sum_{y,b} \phi^a(x) (-\square_{xy}^{ab}) \phi^b(y), \quad (7)$$

where

$$-\square_{xy}^{ab} = \sum_{\mu} [2\delta_{xy} \delta^{ab} - R_{\mu}^{ab}(x) \delta_{y,x+\hat{\mu}} - R_{\mu}^{ba}(y) \delta_{y,x-\hat{\mu}}]. \quad (8)$$

Minimizing Eq. (7) amounts to finding the eigenvector belonging to the lowest eigenvalue of the covariant Laplacian operator. This eigenvalue problem can be solved numerically (we used an implicitly restarted Arnoldi method; for example, see Ref. [24]). The gauge transformation matrix $V(s)$ is defined by

$$V^\dagger(s) \sigma_3 V(s) = \sum_{a=1}^3 \hat{\phi}^a(s) \sigma_a, \quad (9)$$

where

$$\hat{\phi}^a(s) = \rho(s) \phi^a(s), \quad (10)$$

$$\rho^2(s) = \sum_{a=1}^3 (\phi^a(s))^2. \quad (11)$$

In the continuum limit, the LA gauge corresponds to the gauge condition

$$\sum_{\mu} (\partial_{\mu} \mp iA_{\mu}^3) (\rho^2 A_{\mu}^{\pm}) = 0. \quad (12)$$

(3) MAWL gauge [25]. The maximally Abelian Wilson loop (MAWL) gauge is a gauge that maximizes a Wilson loop operator written in terms of Abelian link variables:

$$W_A = \cos \Theta_{\mu\nu}(s), \quad (13)$$

where $\Theta_{\mu\nu}(s) = \theta_{\mu}(s) + \theta_{\nu}(s + \hat{\mu}) - \theta_{\mu}(s + \hat{\nu}) - \theta_{\nu}(s)$. It is achieved by diagonalizing the following operator:

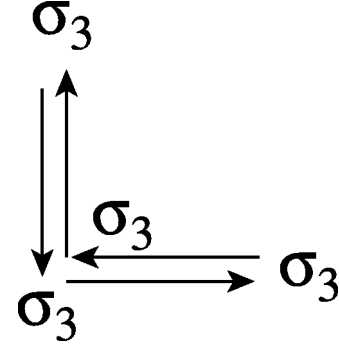


FIG. 4. Schematic representation of L -type gauge.

$$X_{MAWL}(s) = \sum_{\mu \neq \nu} \{ \epsilon(s, \mu) [U(s, \mu) \sigma_3 U^\dagger(s, \mu)] - \epsilon(s - \hat{\mu}, \mu) \times [U^\dagger(s - \hat{\mu}, \mu) \sigma_3 U(s - \hat{\mu}, \mu)] \},$$

where

$$\epsilon(s, \mu) \equiv \frac{\sin \Theta_{\mu\nu}(s) - \sin \Theta_{\mu\nu}(s - \hat{\nu})}{U_0^2(s, \mu) + U_3^2(s, \mu)}.$$

In the continuum limit, we get the following gauge condition:

$$\sum_{\mu \neq \nu} \partial_\nu f_{\mu\nu} A_{\mu}^{\pm} = 0. \quad (14)$$

(4) L -type gauge. There are infinitely many gauges similar to the MA gauge. Here we show one of the simplest extensions called the L -type gauge. It is defined by maximizing

$$R_L = \text{Tr} \sum_{s, \mu \neq \nu} U_{\mu}(s) \sigma_3 U_{\nu}(s + \hat{\mu}) \sigma_3 U_{\nu}^\dagger(s + \hat{\mu}) \sigma_3 U_{\nu}^\dagger(s) \sigma_3.$$

This is given by diagonalizing

$$X_L(s) = \sum_{\mu \neq \nu} [U_{\mu}(s) \sigma_3 U_{\mu}^\dagger(s) \sigma_3 U_{\nu}(s) \sigma_3 U_{\nu}^\dagger(s) + U_{\mu}^\dagger(s - \hat{\mu}) \sigma_3 U_{\nu}(s - \hat{\mu}) \times \sigma_3 U_{\nu}^\dagger(s - \hat{\mu}) \sigma_3 U_{\mu}(s - \hat{\mu})].$$

A schematic representation of R_L is shown in Fig. 4.

In the continuum limit, we get the following gauge condition:

$$\sum_{\mu \neq \nu} \{ (\partial_{\mu} \pm iagA_{\mu}^3) + (\partial_{\nu} \pm iagA_{\nu}^3) \} (A_{\mu}^{\mp} + A_{\nu}^{\mp}) = 0. \quad (15)$$

(5) There are various gauges called the unitary gauge. The Polyakov gauge and F_{12} gauge are defined with the following operators, which are diagonalized:

$$X_{Pol}(s) = \prod_{i=1}^{N_4} U_4(s + (i-1)\hat{4}), \quad (16)$$

$$X_{F_{12}}(s) = U_1(s)U_2(s+\hat{1})U_1^\dagger(s+\hat{2})U_2^\dagger(s), \quad (17)$$

respectively.

In the continuum, the Polyakov gauge is reduced to

$$A_0^\pm(x) = 0, \quad (18)$$

whereas the F_{12} gauge gives

$$F_{12}^\pm(x) = 0. \quad (19)$$

(6) We also consider simple Abelian components extracted without gauge fixing, where exact Abelian dominance is proved analytically [14].

IV. STRING TENSION

As a first step, we measure Abelian and monopole contributions to the string tension in various Abelian projections. We used 100 configurations of a $32^3 \times 16$ lattice for the measurement. In this case, the critical point lies near $\beta_c \sim 2.7$. We set the gauge coupling β to 2.5, so that the system is in the confinement phase. To reduce the statistical errors efficiently, we adapted hypercubic blocking [26] to the original configurations.

The value of Polyakov loop correlators corresponds to the static potential between one pair of quark and antiquark:

$$\langle \text{Tr} P(0) \text{Tr} P^\dagger(R) \rangle = e^{-V(R)/T}, \quad (20)$$

where $P(R)$ is the Polyakov loop operator Eq. (16). $V(R)$ gives the interquark potential

$$V(R) = \sigma R - \frac{\alpha}{R} + c, \quad (21)$$

and $T = 1/(N_4 a)$ is the temperature of the system.

The Abelian Polyakov loop operator is written as

$$P_a = \exp \left[i \sum_{i=0}^{N_4-1} \theta_4(\vec{s} + i\hat{4}) \right]. \quad (22)$$

Equation (22) can be decomposed into photon and monopole parts [11] as follows:

$$P_a = P_p \cdot P_m,$$

$$P_p = \exp \left[-i \sum_{i=0}^{N_4-1} \sum_{s'} D(\vec{s} + i\hat{4} - s') \partial'_\nu \Theta_{\nu 4}(s') \right],$$

$$P_m = \exp \left[-2\pi i \sum_{i=0}^{N_4-1} \sum_{s'} D(\vec{s} + i\hat{4} - s') \partial'_\nu n_{\nu 4}(s') \right],$$

where we use the identity

$$\theta_4(s) = - \sum_{s'} D(s-s') [\partial'_\nu \Theta_{\nu 4}(s') + \partial_4(\partial'_\nu \theta_\nu(s'))].$$

The Abelian field strength tensor

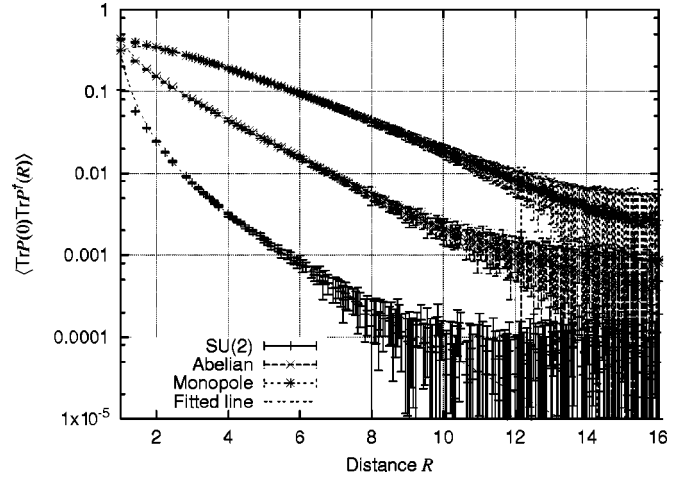


FIG. 5. Abelian and monopole Polyakov loop correlator in the MA gauge.

$$\Theta_{\mu\nu}(s) \equiv \theta_\mu(s) + \theta_\nu(s + \hat{\mu}) - \theta_\mu(s + \hat{\nu}) - \theta_\nu(s)$$

can be decomposed into two parts:

$$\Theta_{\mu\nu}(s) \equiv \bar{\Theta}_{\mu\nu}(s) + 2\pi n_{\mu\nu}(s),$$

where $\Theta_{\mu\nu}(s) \in [-4\pi, 4\pi]$ and $\bar{\Theta}_{\mu\nu}(s) \in [-\pi, \pi]$. Here, $\bar{\Theta}_{\mu\nu}(s)$ is interpreted as the electro-magnetic flux through the plaquette, and the integer valued $n_{\mu\nu}(s)$ corresponds to the number of Dirac strings piercing the plaquette. $D(s-s')$ is the Coulomb propagator on a lattice.

Figures 5, 6, 7, and 8 show the values of $SU(2)$, Abelian, and monopole Polyakov loop correlators in the MA, LA, MAWL, and L -type gauges, respectively. The values of Abelian and monopole Polyakov loop correlators in each gauge are almost degenerate. The string tension σ can be extracted from these values by fitting them to Eq. (20). Fitted lines are also plotted in the same figure. In the case of the MA gauge, the fitted values are consistent with the results by Bali *et al.* [27]. In the case of other gauges like a unitary gauge, one cannot extract the string tension clearly from the Abelian and monopole Polyakov loop correlators due to large statistical errors.

Explicit values of the fitted string tension are shown in Table I. They almost agree with each other, although these four gauges have different gauge fixing conditions in the continuum limit.

V. RG FLOWS OF THE EFFECTIVE ACTION IN VARIOUS ABELIAN PROJECTIONS

To clarify what is happening in the monopole dynamics, we study the effective monopole actions in various gauges in this section.

A. Simulation method

Our method to derive an effective monopole action is the following. We generate $SU(2)$ gauge fields $\{U_\mu(s)\}$ using the standard $SU(2)$ Wilson action. We consider a 48^4 hyper-

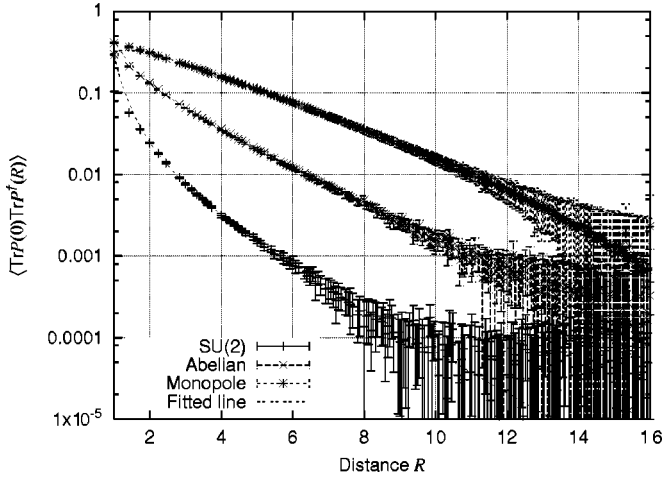


FIG. 6. Abelian and monopole Polyakov loop correlator in the LA gauge.

cubic lattice for β from 2.1 to 2.5. We took 50 independent configurations after 10000 thermalization sweeps. Then, we perform an Abelian projection in six different gauge fixings to extract Abelian gauge fields $\{u_\mu(s)\}$ from $SU(2)$ gauge fields.

One can define magnetic monopole currents from Abelian field strength tensor following DeGrand and Toussaint [28]. We can define the monopole current $k_\mu(s)$ as

$$k_\mu(s) = \frac{1}{2} \epsilon_{\mu\nu\rho\sigma} \partial_\nu n_{\rho\sigma}(s + \hat{\mu}). \quad (23)$$

By definition, it satisfies the current conservation law

$$\partial'_\mu k_\mu(s) = 0,$$

where ∂_μ and ∂'_μ denote the forward and the backward differences, respectively, in the μ direction.

We want to get an effective monopole action $S[k]$ on the dual lattice, integrating out all degrees of freedom except for the monopoles:

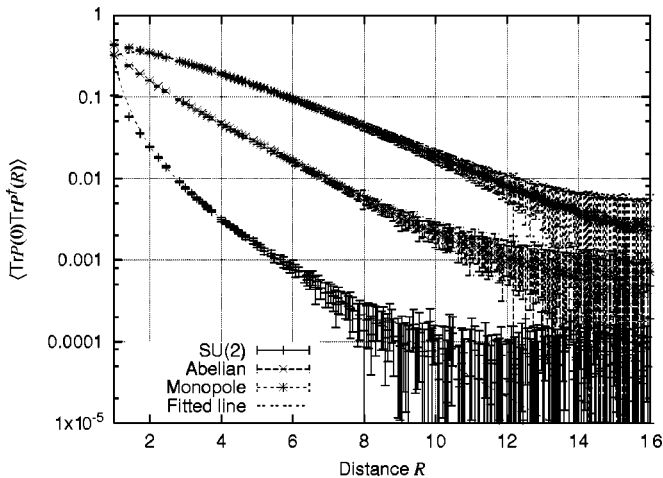


FIG. 7. Abelian and monopole Polyakov loop correlator in the MAWL gauge.

TABLE I. Fitted string tensions ($32^3 \times 16$ lattice, $\beta = 2.5$) $\sigma_{SU(2)} = 0.03446(105)$.

	MA	LA	MAWL	L-type
Abelian	0.03054(45)	0.03011(34)	0.03051(45)	0.03065(43)
Monopole	0.02545(31)	0.02536(28)	0.02546(31)	0.02624(34)

$$\begin{aligned} Z &= \int \mathcal{D}U e^{-S[U]} \delta(X^\pm) \Delta_F(U) \\ &= \int \mathcal{D}u \left[\int \mathcal{D}C e^{-S[U]} \delta(X^\pm) \Delta(U) \right] \\ &= \int \mathcal{D}u e^{-S_{eff}[u]} \\ &= \left(\prod \sum \right) \int \mathcal{D}u e^{-S_{eff}[u]} \delta(k, f(u)) \\ &= \prod_{s, \mu} \sum_{k_\mu(s)=-\infty}^{\infty} \left(\prod_{m, \nu} \delta_{\partial'_\nu k_\nu(m), 0} \right) e^{-S[k]}, \end{aligned}$$

where $U_\mu = C_\mu u_\mu$ and X^\pm is the off-diagonal element of the matrix X which is diagonalized in the procedure of Abelian projection. $\Delta_F(U)$ is the Faddeev-Popov determinant and $\delta(k, f(u))$ gives the definition of the monopole current k as a function of the Abelian gauge field u .

The above integrations are done numerically. We create vacuum ensembles of monopole currents using the Monte Carlo method and the definition of the monopole current Eq. (23). Then, we construct the effective monopole action from monopole vacua using Swendsen's inverse Monte Carlo method, which was developed originally by Swendsen [29] and extended by Shiba and Suzuki [4].

We consider a set of independent and local monopole interactions which are summed up over the whole lattice. We denote each interaction term as $S_i[k]$. Then the effective monopole action can be written as a linear combination of these operators:

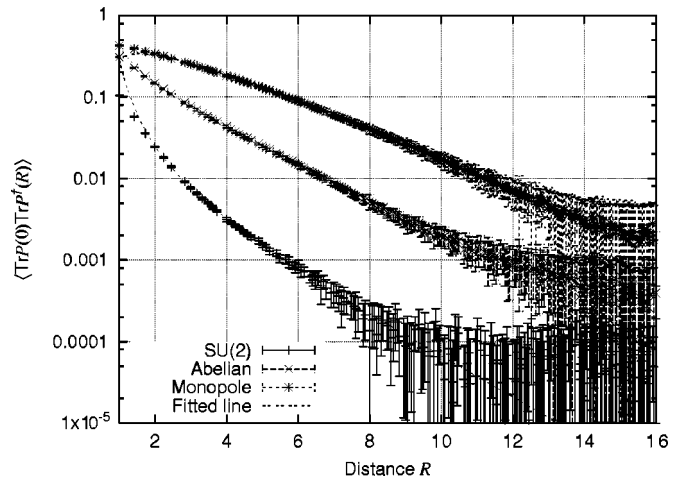


FIG. 8. Abelian and monopole Polyakov loop correlator in the L-type gauge.

TABLE II. The quadratic interactions used for the modified Swendsen method.

Coupling	Distance	Type
g_1	(0,0,0)	$k_\mu(s)$
g_2	(1,0,0)	$k_\mu(s+\hat{\mu})$
g_3	(0,1,0)	$k_\mu(s+\hat{\nu})$
g_4	(1,1,0)	$k_\mu(s+\hat{\mu}+\hat{\nu})$
g_5	(0,1,1)	$k_\mu(s+\hat{\nu}+\hat{\rho})$
g_6	(2,0,0)	$k_\mu(s+2\hat{\mu})$
g_7	(0,2,0)	$k_\mu(s+2\hat{\nu})$
g_8	(1,1,1)	$k_\mu(s+\hat{\mu}+\hat{\nu}+\hat{\rho}+\hat{\sigma})$
g_9	(1,1,1,0)	$k_\mu(s+\hat{\mu}+\hat{\nu}+\hat{\rho})$
g_{10}	(0,1,1,1)	$k_\mu(s+\hat{\nu}+\hat{\rho}+\hat{\sigma})$
g_{11}	(2,1,0,0)	$k_\mu(s+2\hat{\mu}+\hat{\nu})$
g_{12}	(1,2,0,0)	$k_\mu(s+\hat{\mu}+2\hat{\nu})$
g_{13}	(0,2,1,0)	$k_\mu(s+2\hat{\nu}+\hat{\rho})$
g_{14}	(2,1,0,0)	$k_\nu(s+2\hat{\mu}+\hat{\nu})$
g_{15}	(2,1,1,0)	$k_\mu(s+2\hat{\mu}+\hat{\nu}+\hat{\rho})$
g_{16}	(1,2,1,0)	$k_\mu(s+\hat{\mu}+2\hat{\nu}+\hat{\rho})$
g_{17}	(0,2,1,1)	$k_\mu(s+2\hat{\nu}+\hat{\rho}+\hat{\sigma})$
g_{18}	(2,1,1,1)	$k_\mu(s+2\hat{\mu}+\hat{\nu}+\hat{\rho}+\hat{\sigma})$
g_{19}	(1,2,1,1)	$k_\mu(s+\hat{\mu}+2\hat{\nu}+\hat{\rho}+\hat{\sigma})$
g_{20}	(2,2,0,0)	$k_\mu(s+2\hat{\mu}+2\hat{\nu})$
g_{21}	(0,2,2,0)	$k_\mu(s+2\hat{\nu}+2\hat{\rho})$
g_{22}	(3,0,0,0)	$k_\mu(s+3\hat{\mu})$
g_{23}	(0,3,0,0)	$k_\mu(s+3\hat{\nu})$
g_{24}	(2,2,1,0)	$k_\mu(s+2\hat{\mu}+2\hat{\nu}+\hat{\rho})$
g_{25}	(1,2,2,0)	$k_\mu(s+\hat{\mu}+2\hat{\nu}+2\hat{\rho})$
g_{26}	(0,2,2,1)	$k_\mu(s+2\hat{\nu}+2\hat{\rho}+\hat{\sigma})$
g_{27}	(2,2,1,0)	$k_\rho(s+2\hat{\mu}+2\hat{\nu}+\hat{\rho})$

$$S[k] = \sum_i g_i S_i[k], \quad (24)$$

where g_i denotes the effective coupling constants. Explicit forms of the interaction terms are listed in Tables II and III. We determine the set of couplings $\{g_i\}$ from the monopole current ensemble $\{k_\mu(s)\}$ with the aid of an inverse Monte Carlo method. In practice, we have to restrict the number of interaction terms. The form of action adopted here is 27 quadratic interactions and four-point and six-point interactions [5,30].

We perform a block spin transformation in terms of the monopole currents on the dual lattice to study the RG flow. The n -step blocked current is defined by

$$K_\mu(s^{(n)}) = \sum_{i,j,l=0}^{n-1} k_\mu[ns^{(n)} + (n-1)\hat{\mu} + i\hat{\nu} + j\hat{\rho} + l\hat{\sigma}]. \quad (25)$$

The blocked lattice spacing b is given as $b=na(\beta)$ and the continuum limit is taken as the limit $n \rightarrow \infty$ for a fixed physical scale b . We determine the effective monopole action from

TABLE III. The higher order interactions used for the modified Swendsen method.

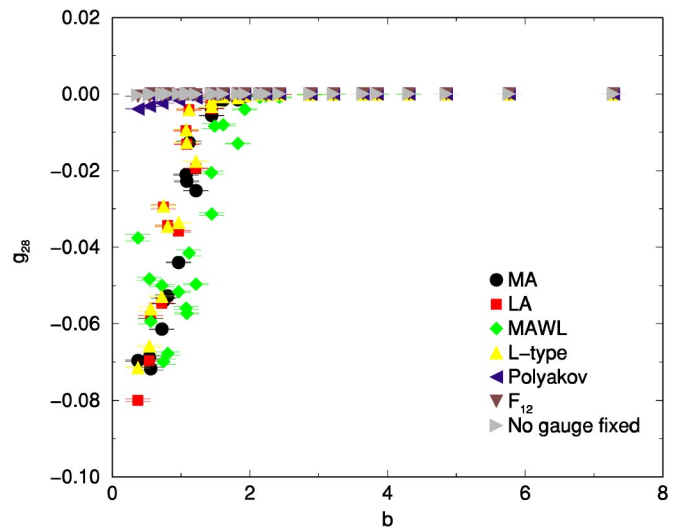
Coupling	Type
Four-point g_{28}	$\sum_s (\sum_{\mu=-4}^4 k_\mu^2(s))^2$
Six-point g_{29}	$\sum_s (\sum_{\mu=-4}^4 k_\mu^2(s))^3$

the blocked monopole current ensemble $\{K_\mu(s^{(n)})\}$. Then one can obtain the RG flow in the 29-dimensional coupling constant space.

B. Numerical results

The effective monopole action is determined successfully. All coupling constants that are contained in the effective monopole action are obtained with relatively small errors. We use the jackknife method for the error estimation. These effective monopole actions except in the MA gauge are determined for the first time in this paper. Moreover, these effective monopole actions are determined from the blocked monopole configurations, too. The results are summarized as follows.

(1) Only the quadratic interaction subspace seems sufficient in the coupling space for the low-energy region of QCD. Figures 9 and 10 show coupling constants for four-point and six-point interaction terms versus physical scale b . Here, note that the effective coupling constants for the blocking factor $n=1$ are omitted in Figs. 9, 10, and 14–23. In the case of the MA, LA, MAWL, and L -type gauges, these coupling constants take relatively larger absolute values for the small b region. They become negligibly small for the large b region. In the case of Polyakov, F_{12} , no gauge fixings, the coupling constants for four-point and six-point interaction terms take the values very close to zero in the whole region of b .

FIG. 9. (Color online) Four-point coupling g_{28} vs physical scale b .

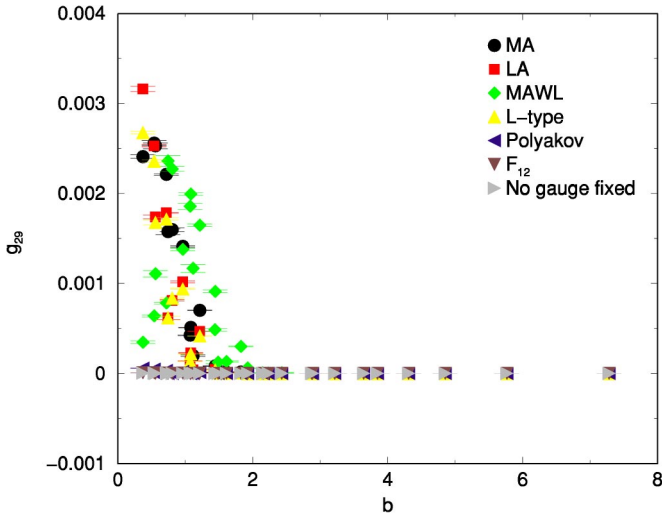


FIG. 10. (Color online) Six-point coupling g_{29} vs physical scale b .

(2) Typical cases of the coupling constants for quadratic interaction terms versus squared distances in lattice units are shown in Fig. 11. We see that the coupling constants for the self-interaction term g_1 and the nearest-neighbor interactions g_2 and g_3 are dominant, and $g_2 \approx g_3$. Other couplings decrease exponentially as the distance between the two monopole currents grows. This behavior does not depend on a gauge coupling constant β . Therefore, we concentrate our analysis on the coupling constants of quadratic interaction terms, especially g_1 and g_2 .

(3) We used a standard iterative gauge fixing procedure for the MA, MAWL, and L -type gauges. In this case, gauge fixing sweeps may be stuck in some local minima of a gauge fixing functional. Different local minima give rise to different gauge transformations, but they cannot be distinguished from the viewpoint of the iterative gauge fixing procedure. These are the lattice Gribov copies. Indeed, Bali *et al.* showed that the effect of such copies on the Abelian string tension is not very small [27]. To check the effect of copies on the effective couplings, we generate 100 $SU(2)$ configurations on a 24^4 lattice at $\beta=2.5$. Then, we generate seven of gauge equivalent configurations (i.e., copies) via a random gauge transformation. Using these gauge copies, we construct effective monopole actions and compare their effective couplings. Fig. 12 shows g_1 in the case of the MA gauge. g_1 for the different blocking factors are described in different symbols. We see some fluctuations in g_1 for the MA gauge. This is nothing but the effect of lattice Gribov copies. The effect of the copies, however, is negligibly small. Therefore, the qualitative analyses that are given later will not be affected. In principle, the LA gauge does not have such copies [8]. Indeed, we confirmed that effective couplings for the LA gauge are not affected by Gribov copies (Fig. 13).

(4) Figures 14 and 15 show the most dominant quadratic self-coupling constant g_1 and quadratic nearest-neighbor coupling constant g_2 versus the physical scale b in the cases of the MA, LA, MAWL, and L -type gauges, respectively. In these gauges, the effective coupling constants take large values in the small b region and the scaling behavior (i.e., the

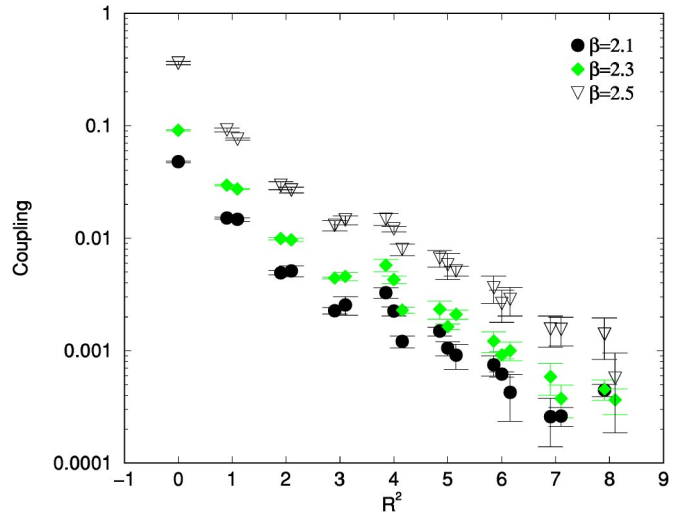


FIG. 11. (Color online) Effective couplings vs squared distances in lattice unit. (MA gauge, $\beta=2.1, 2.3$, and 2.5 , effective couplings for $n=8$ blocked monopole.)

unique curve for different blocking factors n) is seen even in the small b region. The effective actions which are obtained here appear to be a good approximation of the action on the renormalized trajectory corresponding to the continuum limit. In addition to this, the coupling constants for these four gauges are very close to each other, although these gauges have a completely different form in the continuum limit.

(5) However, in the cases of Polyakov, F_{12} and no gauge fixings, the coupling constants are different from those in the above four gauges (see Figs. 16 and 17). In these gauges, coupling constants take smaller values and the scaling behavior is not seen, especially in small b region. To clarify the scaling properties of these coupling constants, we give figures showing a distinction between the different blocking factors n in two typical gauges. In the case of the Polyakov gauge (Fig. 18), the coupling constants depend on the blocking factor n strongly in the small b region. On the other hand, in the case of the LA gauge (Fig. 19), the renormalized coupling constants lie on a unique curve.

(6) Once the effective actions are fixed, we can see from the energy-entropy balance of the system whether monopole condensation occurs or not. If the entropy of a monopole loop exceeds the energy, the monopole loop condenses in the QCD vacuum. In four-dimensional lattice theory, the entropy

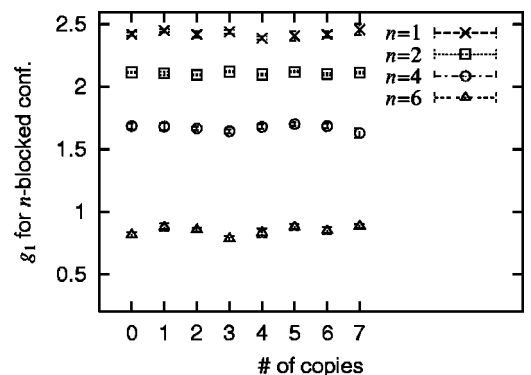


FIG. 12. Gribov copy effect for g_1 (MA gauge).

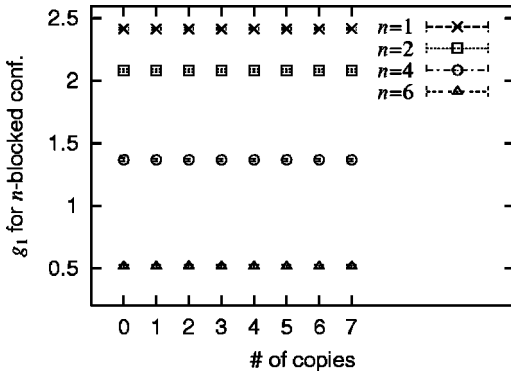


FIG. 13. Gribov copy effect for g_1 (LA gauge).

of a monopole loop can be estimated as $\ln 7$ per unit loop length. It is determined by a random walk without backward tracking. The action can be approximated by the self-interaction term g_1 alone since the interactions with two separate currents are almost canceled [31]. The free energy per unit monopole length is approximated by

$$F \sim g_1 - \ln 7, \tag{26}$$

since g_1 can be regarded as the self-energy per unit monopole loop length. If $g_1 < \ln 7$, the entropy dominates over the energy, that is, monopole condensation occurs. In Figs. 14 and 16, we see that the entropy of the system dominates over the energy in the large b region for all gauges. In other words, monopole condensation occurs [4] in the large b region for all gauges.

(7) Figures 20, 21, 22, and 23 show the RG flows projected onto the g_1 - g_2 , g_1 - g_5 , g_1 - g_7 , and g_1 - g_{10} coupling planes, respectively. The effective coupling constants for all gauges seem to converge to the identical line for the large b region. This may show gauge independence of the monopole condensation in the low-energy region. Although all coupling constants become very small in the large b region, it is important that the slopes of the renormalization flows seem to converge in all gauges.

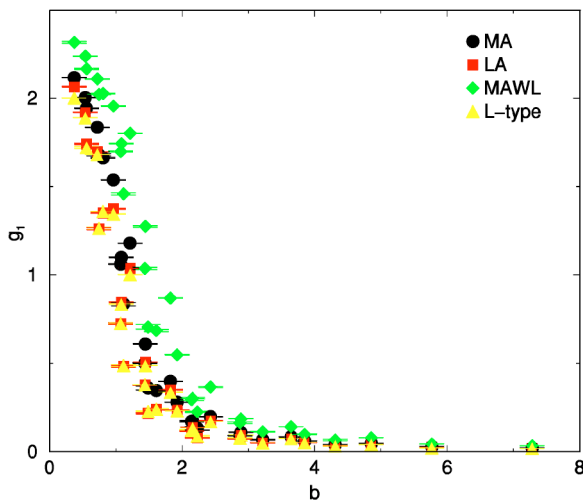


FIG. 14. (Color online) The most dominant self-coupling g_1 vs physical scale b in the MA, LA, MAWL, and L -type gauges.

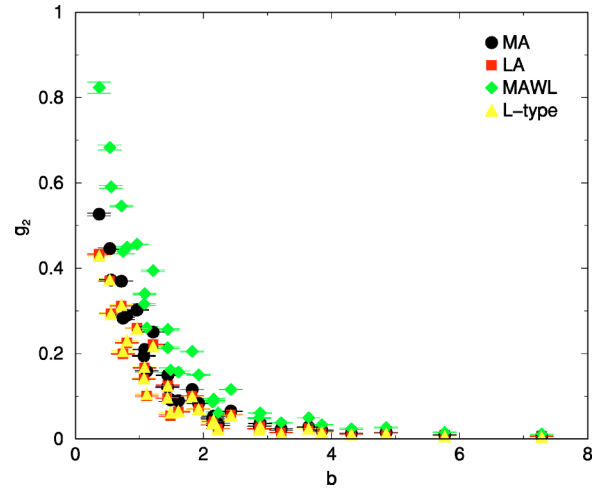


FIG. 15. (Color online) Nearest-neighbor coupling g_2 vs physical b in the MA, LA, MAWL, and L -type gauges.

VI. SUMMARY

We measured first the Abelian and the monopole contributions to the string tension in four types of Abelian projection, i.e., the MA, LA, MAWL, and L -type gauges. They show a good agreement with each other. Similar results for the MA and LA gauges have already been obtained by Ilgenfritz *et al.* in Ref. [32]. Monopole string tensions are extracted in the same manner as Abelian string tensions, and they also agree with each other. The MA and LA gauges are not unique good gauges.

Next, we determined the effective monopole actions in various gauges from monopole vacua using the modified Swendsen method. In the case of the MA gauge, an effective monopole action has already been obtained in Ref. [4]. In addition to this action, the effective monopole actions in the Polyakov gauge, F_{12} gauge, LA gauge, MAWL gauge, L -type gauge, and no gauge fixing are also determined for the first time in this paper. Moreover, these effective actions are determined on the blocked monopole vacua, too. In these

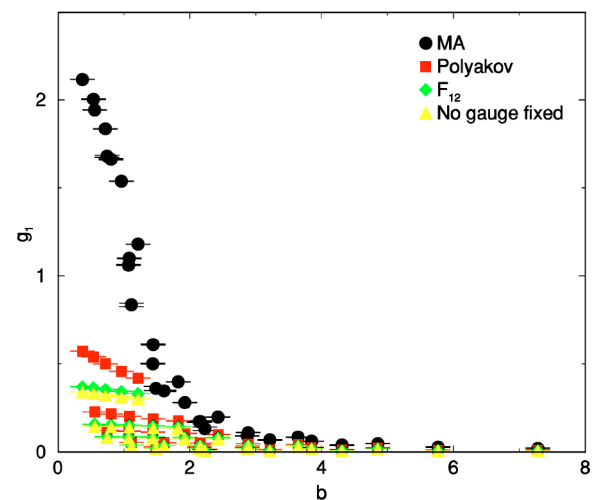


FIG. 16. (Color online) The most dominant self-coupling g_1 vs physical scale b in MA, Polyakov, F_{12} , and no gauge fixings.

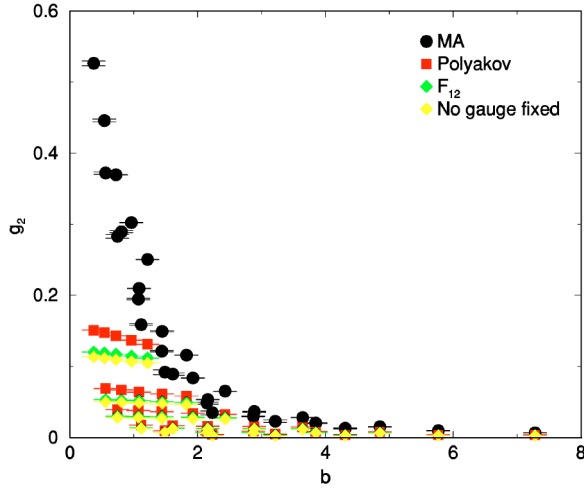


FIG. 17. (Color online) Nearest-neighbor coupling g_2 vs physical scale b in MA, Polyakov, F_{12} , and no gauge fixings.

effective actions, two-point interactions are dominant, whereas four-point and six-point effective coupling constants are negligibly small in the infrared region. The RG flows seem to converge to the identical line when the block spin transformation is repeated. It is important that the slopes of renormalization flows in all gauges seem to converge. The data are compatible with the assumption of gauge independence of the monopole dynamics in the continuum limit. The energy-entropy balance also tells us that monopole condensation occurs in the large b region for all gauges.

ACKNOWLEDGMENTS

The authors would like to thank Fumiyoshi Shoji at Hiroshima University for fruitful discussions. This work was supported by the Supercomputer Project of the Institute of Physical and Chemical Research (RIKEN). Some of our numerical simulations were done using NEC SX-5 at the Research Center for Nuclear Physics (RCNP) of Osaka University.

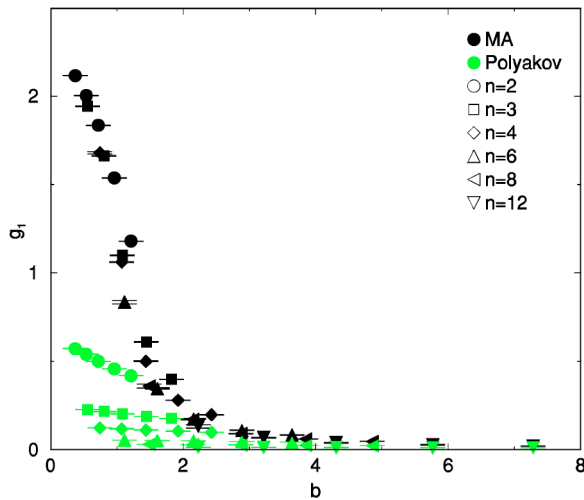


FIG. 18. (Color online) g_1 versus b in the MA and Polyakov gauges. Each symbol corresponds to a different blocking factors n .

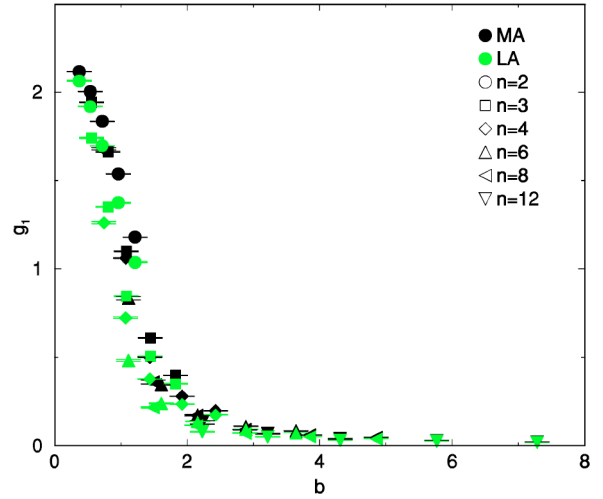


FIG. 19. (Color online) g_1 versus b in the MA and LA gauges. Each symbol correspond to a different blocking factors n .

APPENDIX: MAXIMALLY ABELIAN WILSON LOOP (MAWL) GAUGE

The $SU(2)$ gauge field $U_\mu(s)$ can be parametrized by its isospin components. In this section, we denote each isospin component of $U_\mu(s)$ as $U_0(s, \mu)$, $U_1(s, \mu)$, and so on, for simplicity. This gauge is realized by maximizing the Abelian Wilson loop of 1×1 size:

$$R = \sum_{s, \mu \neq \nu} \cos \Theta_{\mu\nu}(s), \tag{A1}$$

where the Abelian link field is extracted as

$$\theta(s, \mu) = \arctan[U_3(s, \mu)/U_0(s, \mu)]. \tag{A2}$$

Let us consider an infinitesimal gauge transformation of U ,

$$U'(s, \mu) = [1 + i\alpha_i(s)\sigma_i][U_0(s, \mu)I + iU_j(s, \mu)\sigma_j] \times [1 - i\alpha_k(s + \hat{\mu})\sigma_k].$$

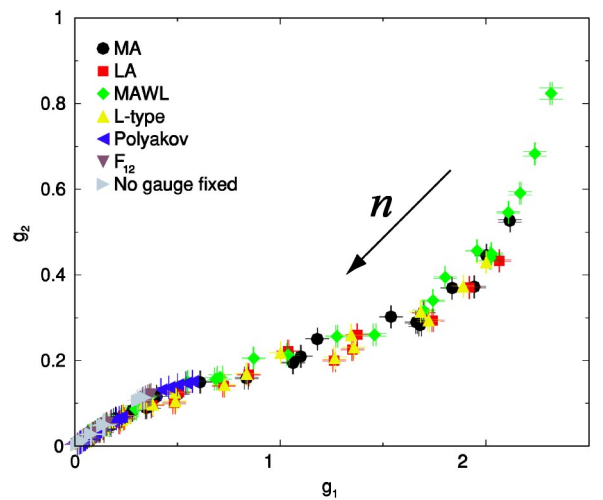


FIG. 20. (Color online) RG flows of effective monopole actions projected onto the g_1 - g_2 coupling plane.

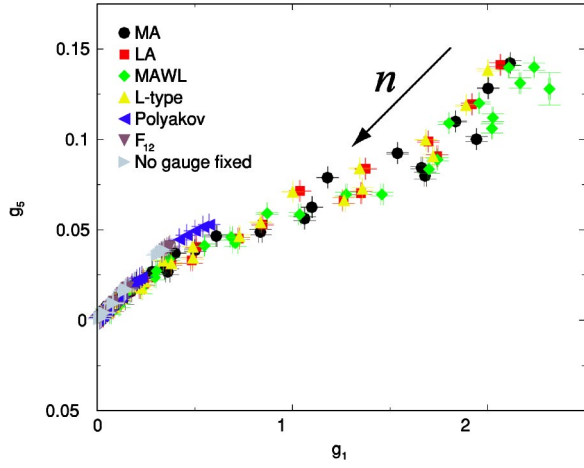


FIG. 21. (Color online) RG flows of effective monopole actions projected onto the g_1 - g_5 coupling plane.

This gives

$$\delta U_0(s, \mu) = -[\alpha_i(s) - \alpha_i(s + \hat{\mu})]U_i(s, \mu), \quad (\text{A3})$$

$$\begin{aligned} \delta U_k(s, \mu) = & [\alpha_k(s) - \alpha_k(s + \hat{\mu})]U_0(s, \mu) \\ & - \epsilon_{ijk}[\alpha_i(s) + \alpha_i(s + \hat{\mu})]U_j(s, \mu). \end{aligned} \quad (\text{A4})$$

Then R changes as

$$\begin{aligned} \delta R = & - \sum_{s, \mu \neq \nu} \sin \Theta_{\mu\nu}(s) \{ \delta \theta(s, \mu) + \delta \theta(s + \hat{\mu}, \nu) \\ & - \delta \theta(s + \hat{\mu}, \mu) - \delta \theta(s, \nu) \}, \end{aligned} \quad (\text{A5})$$

where

$$\delta \theta(s, \mu) = \frac{U_0(s, \mu) \delta U_3(s, \mu) - U_3(s, \mu) \delta U_0(s, \mu)}{U_0^2(s, \mu) + U_3^2(s, \mu)}. \quad (\text{A6})$$

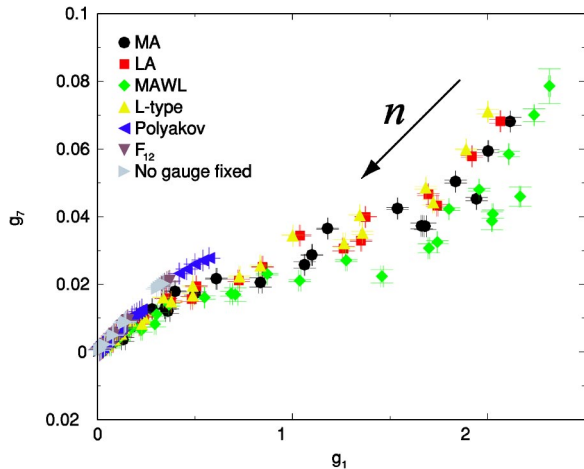


FIG. 22. (Color online) RG flows of effective monopole actions projected onto the g_1 - g_7 coupling plane.

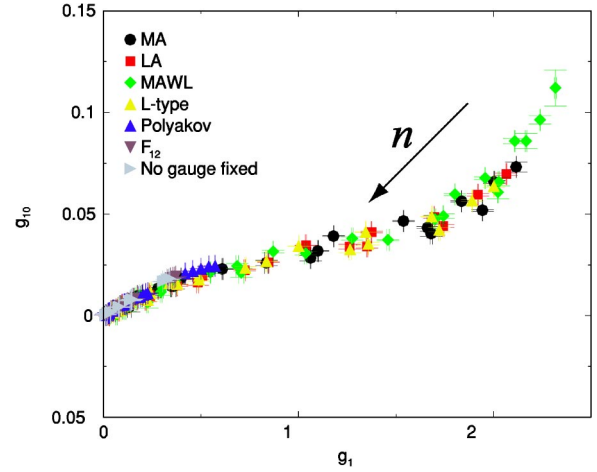


FIG. 23. (Color online) RG flows of effective monopole actions projected onto the g_1 - g_{10} coupling plane.

One can check that R is invariant under the $U(1)$ transformation. Hence we do not need to consider the $\alpha_3(s)$ part. First, let us consider the α_1 part. Since there is a sum over whole lattice sites s , one can shift the site variable, for example, s to $s - \hat{\mu}$. Also one can use the (anti)symmetric property with respect to the μ and ν directions. Finally, one gets

$$-\frac{\delta R}{2} = \sum_{s, \mu \neq \nu} [\alpha_1(s)X_1(s, \mu, \nu) + \alpha_2(s)X_2(s, \mu, \nu)], \quad (\text{A7})$$

$$\begin{aligned} X_1(s, \mu, \nu) = & \epsilon(s, \mu)[U_1(s, \mu)U_3(s, \mu) - U_0(s, \mu)U_2(s, \mu)] \\ & - \epsilon(s - \hat{\mu}, \mu)[U_1(s - \hat{\mu}, \mu)U_3(s - \hat{\mu}, \mu) \\ & + U_0(s - \hat{\mu}, \mu)U_2(s - \hat{\mu}, \mu)], \end{aligned} \quad (\text{A8})$$

$$\begin{aligned} X_2(s, \mu, \nu) = & \epsilon(s, \mu)[U_2(s, \mu)U_3(s, \mu) + U_0(s, \mu)U_1(s, \mu)] \\ & - \epsilon(s - \hat{\mu}, \mu)[U_2(s - \hat{\mu}, \mu)U_3(s - \hat{\mu}, \mu) \\ & - U_0(s - \hat{\mu}, \mu)U_1(s - \hat{\mu}, \mu)], \end{aligned} \quad (\text{A9})$$

where

$$\epsilon(s, \mu) = \frac{\sin \Theta_{\mu\nu}(s) - \sin \Theta_{\mu\nu}(s - \hat{\nu})}{U_0^2(s, \mu) + U_3^2(s, \mu)}. \quad (\text{A10})$$

When we write $X^\pm = X_1 \pm iX_2$, it is easy to see that X^\pm transforms covariantly under the residual $U(1)$.

Finally, one gets the matrix which is diagonalized in this gauge,

$$\begin{aligned} X(s) = & \sum_{\mu \neq \nu} \{ \epsilon(s, \mu)[U(s, \mu)\sigma_3 U^\dagger(s, \mu)] - \epsilon(s - \hat{\mu}, \mu) \\ & \times U^\dagger(s - \hat{\mu}, \mu)\sigma_3 U(s - \hat{\mu}, \mu) \}. \end{aligned}$$

Because of the nonlocality of the gauge condition, one cannot calculate the gauge transformation matrix that diagonalizes $X(s)$ in a simple way. Therefore, we employed an iterative update procedure to satisfy the gauge condition.

(1) Make a trial gauge transformation, adopting α_1 and α_2 as follows: $\alpha_1(s) = -\kappa X_1(s)$, $\alpha_2(s) = -\kappa X_2(s)$.

(2) Measure R . If R becomes larger than before, accept this trial and repeat step 1. If R becomes smaller than before, take $\kappa_{new} = \kappa_{old}/2$ and adopt the gauge transformation using this κ_{new} with respect to the configuration before trial, and then repeat step 1.

(3) If the off-diagonal element of $X(s)$ becomes smaller than a suitable threshold (we set this to 1.0), one can regard the gauge fixing procedure as having been completed.

We set the initial value of κ to 0.1. R can be maximized as long as we take $\kappa > 0$. We apply the MA gauge fixing as a preconditioning for the MAWL gauge fixing and then we perform the above procedure on the MA fixed configuration. This preconditioning is required to improve the convergence property of the MAWL gauge fixing. We have to note that the configurations obtained via the above procedure are not perfectly gauge fixed because the off-diagonal elements of $X(s)$ still remain not very small.

-
- [1] G. 't Hooft, in *High Energy Physics*, edited by A. Zichichi (Editorice Compositori, Bologna, 1976).
- [2] S. Mandelstam, *Phys. Rep.* **23C**, 245 (1976).
- [3] G. 't Hooft, *Nucl. Phys.* **B190**, 455 (1981).
- [4] H. Shiba and T. Suzuki, *Phys. Lett. B* **343**, 315 (1995); **351**, 519 (1995), and references therein.
- [5] M. N. Chernodub *et al.*, *Phys. Rev. D* **62**, 094506 (2000).
- [6] Gunnar S. Bali, Christoph Schlichter, and Klaus Schilling, *Prog. Theor. Phys. Suppl.* **131**, 645 (1998).
- [7] Y. Koma, E.-M. Ilgenfritz, T. Suzuki, and H. Toki, *Phys. Rev. D* **64**, 014015 (2001).
- [8] A. J. van der Sijs, *Prog. Theor. Phys. Suppl.* **131**, 149 (1998).
- [9] A. J. van der Sijs, *Nucl. Phys. B (Proc. Suppl.)* **73**, 548 (1999).
- [10] T. Suzuki and I. Yotsuyanagi, *Phys. Rev. D* **42**, 4257 (1990); *Nucl. Phys. B (Proc. Suppl.)* **B20**, 236 (1999).
- [11] Shinji Ejiri, Shun-ichi Kitahara, Yoshimi Matsubara, Tsuyoshi Okude, Tsuneo Suzuki, and Koji Yasuta, *Nucl. Phys. B (Proc. Suppl.)* **47**, 322 (1996).
- [12] F. Shoji, T. Suzuki, H. Kodama, and A. Nakamura, *Phys. Lett. B* **476**, 199 (2000).
- [13] Tsuneo Suzuki, Sawut Ilyar, Yoshimi Matsubara, Tsuyoshi Okude, and Kenji Yotsuji, *Phys. Lett. B* **347**, 375 (1995); **351**, 603(E) (1995).
- [14] M. C. Ogilvie, *Phys. Rev. D* **59**, 074505 (1999).
- [15] John D. Stack, Steven D. Neiman, and Roy J. Wensley, *Phys. Rev. D* **50**, 3399 (1994).
- [16] H. Shiba and T. Suzuki, *Phys. Lett. B* **333**, 461 (1994).
- [17] K. Yamagishi, S. Kitahara, S. Ito, T. Tsunemi, S. Fujimoto, S. Kato, F. Shoji, T. Suzuki, H. Kodama, and A. Nakamura, *Nucl. Phys. B (Proc. Suppl.)* **83**, 550 (2000).
- [18] V. L. Beresinskii, *Sov. Phys. JETP* **32**, 493 (1970).
- [19] J. M. Kosterlitz and D. J. Thouless, *J. Phys. C* **6**, 1181 (1973).
- [20] A. Di Giacomo, hep-lat/0206018, and references therein.
- [21] O. Jahn and F. Lenz, *Phys. Rev. D* **58**, 085006 (1998).
- [22] M. N. Chernodub, F. V. Gubarev, M. I. Polikarpov, and A. I. Veselov, *Prog. Theor. Phys. Suppl.* **131**, 309 (1999).
- [23] Shinji Ejiri, Shun-ichi Kitahara, Yoshimi Matsubara, and Tsuneo Suzuki, *Phys. Lett. B* **343**, 304 (1995).
- [24] See url <http://www.caam.rice.edu/software/ARPACK/>
- [25] Tsuneo Suzuki, Yoshimi Matsubara, Shun-ichi Kitahara, Shinji Ejiri, Naoki Nakamura, Fumiyooshi Shoji, Masafumi Sei, Seikou Kato, and Natsuko Arasaki, *Nucl. Phys. B (Proc. Suppl.)* **53**, 531 (1997).
- [26] A. Hasenfratz and F. Knechtli, *Phys. Rev. D* **64**, 034504 (2001).
- [27] G. S. Bali, V. Bornyakov, M. Mueller Preussker, and K. Schilling, *Phys. Rev. D* **54**, 2863 (1996).
- [28] T. A. DeGrand and D. Toussaint, *Phys. Rev. D* **22**, 2478 (1980).
- [29] R. H. Swendsen, *Phys. Rev. Lett.* **52**, 1165 (1984); *Phys. Rev. B* **30**, 3866 (1984).
- [30] Maxim N. Chernodub, Seikou Kato, Naoki Nakamura, Mikhail I. Polikarpov, and Tsuneo Suzuki, hep-lat/9902013.
- [31] Shun-ichi Kitahara, Yoshimi Matsubara, and Tsuneo Suzuki, *Prog. Theor. Phys.* **93**, 1 (1995).
- [32] E.-M. Ilgenfritz, S. Thurner, H. Markum, and M. Müller-Preussker, *Phys. Rev. D* **61**, 054501 (2000).